MINISTRY OF EDUCATION AND TRAINING
VIETNAM ACADEMY OF SCIENCE AND TECHNOLOGY

GRADUATE UNIVERSITY OF SCIENCE AND TECHNOLOGY

Le Trong Duc

SYNTHESIS, STRUCTURAL STUDY, AND BIOLOGICAL ACTIVITY OF SOME HETEROCYCLIC COMPOUNDS DERIVED FROM 2-(NAPHTHALEN-1-YL)ACETIC ACID

SUMMARY OF DISSERTATION ON SCIENCES OF MATTER

Major: Organic Chemistry

Code: 9 44 01 14

The dissertation is completed at: Graduate University of Science and Technology, Vietnam Academy Science and Technology

Supervisors:

1. Supervisor 1: Assoc. Prof. Dr. Nguyen Tien Cong
   Ho Chi Minh City University of Education
2. Supervisor 2: Assoc. Prof. Dr. Hoang Thi Kim Dung
   Institute of Advanced Technology

Referee 1:.....

Referee 2:.....

Referee 3:.....

The dissertation is examined by Examination Board of Graduate University of Science and Technology, Vietnam Academy of Science and Technology at…….. (time, date……)

The dissertation can be found at:

1. Graduate University of Science and Technology Library
2. National Library of Vietnam

INTRODUCTION

1. Reasons for the topic choice

Recent studies have shown that heterocyclic compounds are increasingly attracting interest due to their diverse biological activities, particularly five-membered nitrogen-containing heterocycles such as pyrrole, imidazole, triazole, oxadiazole, and thiazolidine. These compounds have promising pharmaceutical applications owing to their antibacterial, antifungal, anti-inflammatory, antiviral, antidiabetic, anticonvulsant, antioxidant, and anticancer properties.

1,2,4-Triazole derivatives exhibit significant biological activities, especially in α-glucosidase enzyme inhibition and malignant tumor therapy. Several drugs containing this heterocycle, such as fluconazole, voriconazole, and itraconazole (antifungal), alprazolam (anticonvulsant), ribavirin (antiviral), letrozole, and anastrozole (aromatase inhibitors), highlight the therapeutic potential of 1,2,4-triazole in medicine.

The 2-thioxothiazolidin-4-one compound, particularly its 5-arylidene derivatives, shows promise in diabetes treatment and possesses antibacterial, antifungal, antitubercular, and anticancer activities. Meanwhile, naphthalene and its derivatives exhibit antibacterial, antiviral, anti-inflammatory, anticancer, antipsychotic, antidepressant, and neuroprotective effects. Additionally, 2-(naphthalen-1-yl)acetic acid is used as a fungicide and plant growth regulator.

Despite extensive research on heterocyclic compounds, studies on derivatives of 2-(naphthalen-1-yl)acetic acid remain limited, particularly regarding their structure and biological activities. Therefore, this study focuses on the synthesis and investigation of 2-thioxothiazolidin-4-one and 1,2,4-triazole derivatives from 2-(naphthalen-1-yl)acetic acid to evaluate their structures, properties, and biological activities.

2. Research Objectives

- Synthesize heterocyclic compounds containing 2-thioxothiazolidin-4-one and 1,2,4-triazole.

- Determine the structures of the synthesized compounds using modern spectroscopic methods such as FT-IR, ^{1}H-NMR, ^{13}C-NMR, and HR-MS.

- Confirm the structures of selected compounds with suitable crystals using single crystal X-ray diffraction.

- Investigate the α-glucosidase inhibitory activity of the synthesized compounds (*in vitro* and *in silico*).

3. Research Content

- Synthesizing new heterocyclic compounds derived from 2-(naphthalen-1-yl)acetic acid. Based on the research objective, these heterocyclic compounds are categorized into two groups with three series:

+ The first group consists of derivatives at position 5th of the 2-thioxothiazolidin-4-one ring, specifically 2-(naphthalen-1-yl)-*N*-(4-oxo-2-thioxothiazolidin-3-yl)acetamide.

+ The second group includes two series of compounds containing the 1,2,4-triazole ring:

- The first series includes 2-{[5-(naphthalen-1-ylmethyl)-4-phenyl/ethyl-4*H*-1,2,4-triazol-3-yl]thio}-*N*-aryl acetamide derivatives.
- The second series includes 2-{[5-(naphthalen-1-ylmethyl)-4-phenyl/ethyl-4*H*-1,2,4-triazol-3-yl]thio}-1-aryl ethane-1-one derivatives.

- Investigating the physical properties (state, color, crystallization solvent, melting point) of the synthetic compounds.

- Characterizing the structures of synthesized compounds using modern spectroscopic techniques such as FT-IR, NMR, and high-resolution

mass spectrometry (HR-MS).

- Determining the crystal structures of selected compounds with suitable crystals via single-crystal X-ray diffraction.

- Evaluating the α-glucosidase inhibitory activity of the synthesized compounds and analyzing the structure-activity relationship (SAR).

- Performing molecular docking studies of the synthetic compounds on the target enzyme α-glucosidase (PDB ID: 6C9X).

4. New contributions of the thesis

- Synthesized 42 compounds including intermediates and compounds containing heterocycles 2-thioxothiazolidin-4-one and 1,2,4-triazole from 2-(napthalen-1-yl)acetic acid. Of these, 39 are new compounds according to SciFinder August 2025.

- Study the structure and properties of synthesized compounds by methods of determining melting point, crystallization solvent, modern spectroscopic methods such as: FT-IR, NMR, HR-MS and single crystal X-ray diffraction.

- Evaluate the enzyme α-glucosidase inhibitory activity of 39 new compounds, and explain the enzyme inhibition mechanism by molecular docking method, compared with the reference compound (voglibose).

5. Layout

The thesis consists of 138 pages, introduction 3 pages; overview 26 pages; experimental 10 pages; results and discussion 82 pages; conclusion and recommendations 2 pages. The thesis has 104 figures and 38 tables; references 14 pages with 129 documents. In addition, there is an appendix with spectra images.

CHAPTER 1. OVERVIEW

A comprehensive review of domestic and international literature on the synthesis and biological activities of heterocyclic compounds containing 1,2,4-triazole and 2-thioxothiazolidin-4-one has been conducted. The review highlights highlights these two heterocyclic groups, multiple synthesis methods, and their biological activities, including α-glucosidase enzyme inhibition, antibacterial, antifungal, antitubercular, cytotoxic effects on certain cancer cell lines, anti-inflammatory, and hypoglycemic properties, among others. Additionally, the review indicates that research on these heterocycles represents a growing trend, attracting significant interest and rapid development. However, studies focusing on the synthesis of these two heterocycles from 2-(naphthalen-1-yl)acetic acid remain limited. This serves as the foundation for selecting the research topic on the synthesis, structural investigation, and biological evaluation of certain heterocyclic compounds, with the aim of creating novel compounds and identifying those with strong biological activities that hold potential applications in pharmaceutical chemistry.

CHAPTER 2. EXPERIMENT

2.1. Methods of studying the structure and properties

The synthesized compounds were characterized and structured by the following methods: Melting point (measured by capillary method), infrared spectrum (FT-IR, measured by pelleting method with KBr), nuclear magnetic resonance spectrum (^{1}H-NMR, ^{13}C-NMR, recorded on Bruker Avance (Germany) using DMSO-d_6), mass spectrum (HR-MS, measured by ESI method, on Bruker micrOTOF-Q 10187 spectrometer (Germany), X-ray single crystal diffraction spectrum (measured on Agilent SuperNova X-ray diffractometer and on Bruker D8 Quest).

2.2. Synthesis of compounds

Compounds containing heterocyclic 2-thioxothiazolidin-4-one and 1,2,4-triazole were synthesized from the starting material 2-(naphthalen-1-yl)acetic acid as described in Figure 2.1 (page 6).

2.3. α-glucosidase enzyme inhibitory activity assay

2.3.1. Method for testing the enzyme inhibitory activity of α-glucosidase

Enzyme inhibitory activity was performed at the Laboratory of Experimental Biology, Institute of Natural Products Chemistry, Vietnam Academy of Science and Technology according to the method for rapid determination of α-glucosidase enzyme inhibitory activity based on the hydrolysis reaction of the substrate *p*-nitrophenyl-α-D-glucopyranoside (*p*NPG).

2.3.2. Molecular docking method

Docking is one of the most popular methods used in structure-based drug design because it is capable of predicting with high accuracy the formation of ligand-receptor binding in the binding pocket. In the framework of this thesis, the molecular docking method is used to explain the mechanism of action of compounds on the enzyme α-glucosidase. The

docking process is carried out through three steps:

- Protein preparation: the 3D structure of the enzyme α-glucosidase was downloaded from the Protein Data Bank (PDB ID: 6C9X, rcsb.org).

- Ligand preparation:

+ Prepare 3 types of ligand for re-docking.

+ Prepare ligands which are synthetic substances for docking.

- Docking simulation: performed on AutoDock Vina 1.2.3 software. Interactions between proteins and ligands from docking poses were analyzed using PyMOL software.

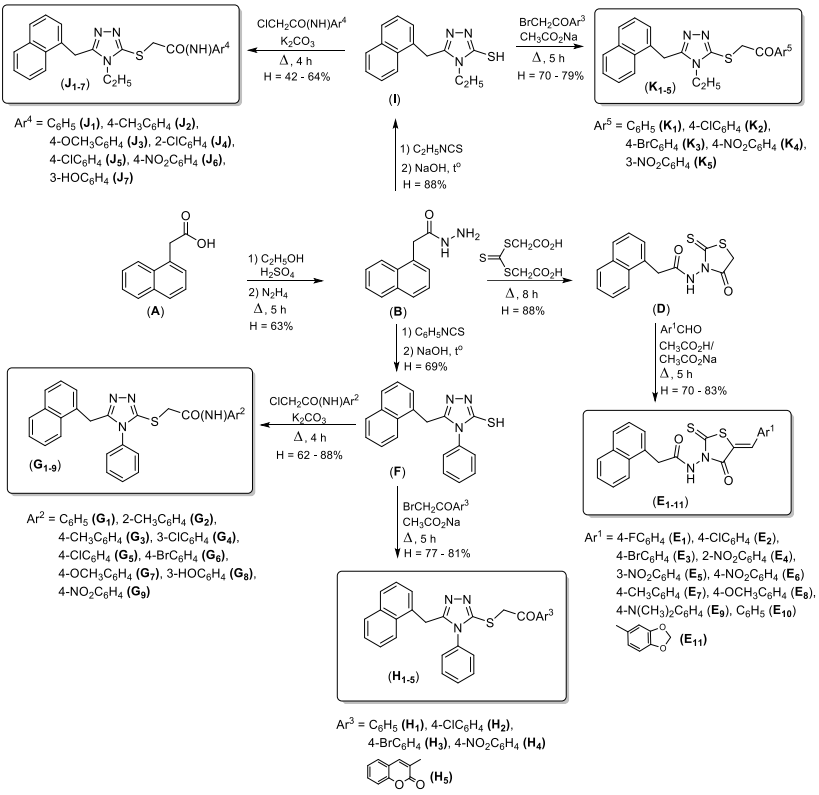

Figure 2.1. Synthesis of compounds containing thiazolidine and 1,2,4-triazole heterocycles

CHAPTER 3. RESULTS AND DISCUSSION

3.1. Synthesis and bioactivity of compounds containing heterocyclic 2-thioxothiazolidin-4-one

3.1.1. Synthetic

Compounds containing the heterocyclic 2-thioxothiazolidin-4-one (**D**, $\mathbf{E_{1\text{-}11}}$) were synthesized from 2-(naphthalen-1-yl)acetohydrazide (**B**) as described Figure 2.1.

3.1.1.1. Synthetic processes

- Synthesis of 2-(naphthalen-1-yl)acetohydrazide (**B**) is presented in section 2.3.1 of the thesis.

- Synthesis of 2-(naphthalen-1-yl)-*N*-(4-oxo-2-thioxothiazolidin-3-yl)acetamide (**D**) is presented in section 2.3.2.1 of the thesis.

- Synthesis of *N* -(5-arylidene-4-oxo-2-thioxothiazolidin-3-yl)-2-(naphthalen-1-yl)acetamide ($\mathbf{E_{1\text{-}11}}$) by refluxing compound (**D**) with aromatic aldehydes, in the presence of CH_3COONa in acetic acid solvent, presented in section 2.3.2.2 of the thesis.

3.1.1.2. Result

- Compound (**B**) is presented in section 3.1 of the thesis.

- Compound (**D**) is presented in section 3.2.1 of the thesis.

- The series of compounds ($\mathbf{E_{1\text{-}11}}$) were synthesized through the Knoevenagel condensation reaction between compound (**D**) and aromatic aldehydes. The synthesis results and some physical properties are summarized in table 3.1, the results of IR, ^{1}H-NMR, ^{13}C-NMR, HR-MS spectra are presented in tables 3.4 to 3.7 of the thesis. The X-ray data are presented in table 3.8, figures 3.17 to 3.18 of the thesis.

Table 3.1. Results of synthesis of compounds ($\mathbf{E_{1\text{-}11}}$)

Compounds	Solvent recrystallize	Melting point (^{o}C)	Status – color	Yield (%)
$\mathbf{E_1}$	AcOH : H_2O	157	Yellow crystals	78.2
$\mathbf{E_2}$	AcOH : H_2O	188	White crystals	76.9

E_3	AcOH : H_2O	156	Yellow crystals	81.0
E_4	AcOH : H_2O	168	Yellow crystals	79.6
E_5	AcOH : H_2O	171	Yellow crystals	75.3
E_6	AcOH : H_2O	185	Yellow crystals	82.1
E_7	AcOH : H_2O	153	Yellow crystals	83.3
E_8	AcOH : H_2O	162	Yellow crystals	74.5
E_9	AcOH : H_2O	164	Red brown crystals	70.2
E_{10}	AcOH : H_2O	166	Yellow crystals	79.6
E_{11}	AcOH : H_2O	177	Moss green crystals	75.8

3.1.1.3. Structure

The structures of the compounds (**D**, **E_{1-11}**) were confirmed by FT-IR, ^{1}H-NMR, ^{13}C-NMR, HR-MS spectroscopy. Some compounds with suitable crystals (**D**, **E_4**, **E_8**) were analyzed by X-ray diffraction. The results showed that all compounds had good agreement between the expected structure and the spectral data. The signals on the NMR spectrum also helped confirm that the series of compounds (**E_{1-11}**) existed in the (*Z*)-configuration and the X-ray diffraction method also confirmed the (*Z*)-configuration of these compounds once again.

The IR spectrum of compound **D** shows typical absorption signals, consistent with the expected structure. The characteristic absorptions for this compound are at 3163 cm $^{-1}$ (>N–H), 1667 cm $^{-1}$ (C=O amide) and especially compared to compound **B**, this compound **D** has an additional signal at 1753 cm^{-1} proving the existence of C=O in the 2-thioxothiazolidin-4-one component, indicating that the chemical reaction has occurred successfully. On the ^{1}H-NMR spectrum of compound **D** showed a total of 12 protons, and the ^{13}C-NMR spectrum of the compound showed a total of 15 signals consistent with the predicted structure. The signal at δ 200.6 ppm was attributed to the carbon of the C=S attached to the thiazolidine heterocycle, the signals at δ 170.7 ppm and 169.1 ppm were attributed to the carbon of the C=O group.

Similar to the IR spectrum of compound **D**, this series of compounds

E$_{1\text{-}11}$ also shows characteristic signals for vibrations of N–H bonds, Csp^2–H, Csp^3–H, C=O, C=C, C=S and C=N. Compared with the signal of the C=O group on the 2-thioxothiazolidin-4-one ring of compound **D** (1753 cm^{-1}), the signal of the C=O group on the 2-thioxothiazolidin-4-one ring in compounds **E**$_{1\text{-}11}$ participates in the conjugation system with the arylidene component, so it appears at a lower frequency (1717 – 1742 cm^{-1}).

^{1}H-NMR spectrum of compounds **E**$_{1\text{-}11}$ (see the example spectrum of compound **E**$_1$ in Figure 3.1), all signals appeared as expected. The methylene group outside the thiazolidine ring (–CH_2CONH–) still appeared with a *singlet* signal at δ 4.18 – 4.24 ppm while the signal of the methylene group inside the thiazolidine ring disappeared, at the same time, the spectrum also showed additional signals in the aromatic ring (δ 6.17 – 8.54 ppm) demonstrating the successful formation of compounds **E**$_{1\text{-}11}$. In addition, the *singlet* signal of the methylidene group in the **E**$_{1\text{-}11}$ series (δ 7.76 – 8.18 ppm) also appeared in the spectrum and played an important role in determining the *E*/*Z* configuration of these compounds .

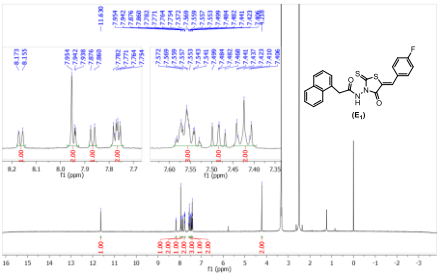

Figure 3.1. ^{1}H-NMR spectrum of compound E$_1$

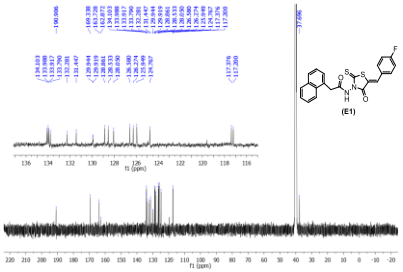

Figure 3.2. ^{13}C-NMR spectrum of compound E$_1$

In the NMR spectra of compounds **E**$_{1\text{-}11}$, only a single proton signal corresponding to the methylene group is observed, indicating that these compounds exist exclusively in either the *Z* or *E* isomeric form. The proton signal of the methylene group in *Z* and *E* isomers differs in chemical shift: compared to the *E* isomer, the proton signal in the *Z* isomer shifts downfield.

This trend has been previously recorded in (*Z*)-5-(pyridin-2-ylmethylene)-2-thioxothiazolidin-4-one and (*Z*)-3-allyl-5-(4-nitrobenzylidene)-2-sulfanylidene-1,3-thiazolidin-4-one, where the methylene proton signals in their ^{1}H-NMR spectra (DMSO-d_6) appear at δ 7.70 ppm and δ 7.93 ppm, respectively.

Conversely, for the *E* isomer, a series of (*E*)-5-[(1-phenyl-1*H*-1,2,3-triazol-4-yl)methylene]-2-thioxothiazolidin-4-one compounds synthesized by Venkatakrishna Manikala et al. showed that the methylene proton signal appears in a higher field region, around δ 7.12–7.62 ppm. In the **E$_{1\text{-}11}$** compound series, the methylene proton signals also appear in a low-field region, with chemical shifts ranging from δ 7.76 to 8.18 ppm, similar to those of *Z*-configured compounds in the aforementioned examples. This evidence supports the conclusion that the exocyclic double bond in the thiazolidine ring adopts a (*Z*)-configuration. Furthermore, the preference for the (*Z*) configuration can be rationalized based on thermodynamic stability, as discussed in the literature.

In addition, on the ^{13}C-NMR spectrum, there are also signals of the methylene group directly attached to the naphthalene ring at δ 36.6 - 37.8 ppm and signals of the methyl group in compounds **E$_7$**, **E$_8$**, **E$_9$** at δ 21.7 ppm, 56.1 ppm, 21.5 ppm, respectively. In which, the signal of the methyl group in compound **E$_8$** is directly attached to the highly electronegative oxygen atom, so it shifts to a weaker magnetic field region, corresponding to a higher shift than the carbon signals of the methyl group in compounds **E$_7$** and **E$_9$**.

The high-resolution mass spectrum HR-MS of compounds **E$_{1\text{-}11}$** also showed molecular ion peaks consistent with the expected structures, confirming that the series of compounds **E$_{1\text{-}11}$** were successfully synthesized.

By X-ray diffraction, the crystal structures of **E$_4$** and **E$_8$** were confirmed to exist in the (*Z*) configuration of the outer double bond of the thiazolidine ring, as indicated by the signals of the methylidene group

(–CH=) in the ^{1}H-NMR spectrum. A search in the Cambridge Structure Database (CSD, version 5.45, updated June 2024) show that 223 out of 241 structures exhibit the (*Z*)-configuration.

3.1.2. α-glucosidase enzyme inhibitory activity

All tested compounds (except compounds **D**, **E$_5$,** and **E$_8$**) exhibited significant inhibitory potency (Figure 3.3, Table 3.2), with IC_{50} values ranging from 7.5 ± 0.5 µM to 290.3 ± 1.9 µM, demonstrating greater inhibition than voglibose (IC_{50} = 355.8 ± 3.5 µM) .

Table 3.2. Inhibitory activity of α-glucosidase enzyme of compound series (D, E$_{1-11}$)

Compounds	R	IC $_{50}$ (µM)	Binding energy (kcal/mol)	Hydrogen bond
D		-	-7.0	-
E$_1$	4-F	155.9 ± 2.7	-8.7	Asp420
E$_2$	4-Cl	7.5 ± 0.5	-8.1	Asp73
E$_3$	4-Br	100.8 ± 2.5	-8.4	Asp420
E$_4$	2-NO_2	71.9 ± 1.6	-8.5	Asp420
E$_5$	3-NO_2	-	-8.9	Asp420
E$_6$	4-NO_2	149.9 ± 2.4	-8.7	Asp420
E$_7$	4-CH_3	19.9 ± 0.5	-8.8	Asp73
E$_8$	4-OCH_3	-	-8.4	His478
E$_9$	4-$N(CH_3)_2$	65.3 ± 2.5	-8.1	Asp420
E$_{10}$	H	290.3 ± 1.9	-8.0	Asp73
E$_{11}$		37.3 ± 1.8	-9.7	His478
Voglibose		355.8 ± 3.5		

Note: (-) does not represent activity/no hydrogen bonding

The presence or absence of substituents, as well as the properties of the substituents (electron-donating, electron-withdrawing) at position 5th of the thiazolidine ring

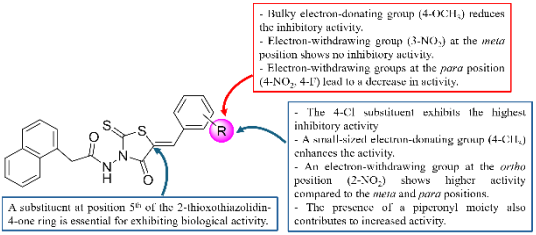

Figure 3.3. Structure–activity relationship of compounds E$_{1–11}$

significantly affected the α-glucosidase inhibitory activity of these compounds. Compound **D**, which lacked a substituent at this position, showed no activity, which again emphasizes the important role of substituents in α-glucosidase inhibition.

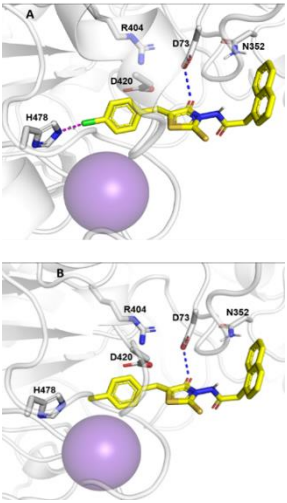

Figure 3.4. Docking poses of compounds E_2 (A) and E_7 (B)

Among the halogen-containing compounds, $\mathbf{E_2}$ (4-Cl) demonstrates the strongest inhibitory activity, as the electron-withdrawing nature of chlorine enhances enzyme inhibition. The activity follows the trend: 4-Cl > 4-Br > 4-F. Small electron-donating groups such as 4-CH_3 enhance activity, whereas bulkier groups like 4-OCH_3 reduce effectiveness due to steric hindrance. Additionally, the nitro group at the *ortho* position improves activity, while at the *meta* position, it loses its effect, highlighting the importance of substituent orientation in optimizing enzyme inhibition.

Docking studies (see Figure 3.4) reveal that compound **D** exhibits weak affinity for α-glucosidase due to the lack of critical hydrogen bonds. $\mathbf{E_2}$ (4-Cl) achieves stable binding through hydrogen bonding with Asp73 and halogen bonding with His478. In contrast, $\mathbf{E_1}$ (4-F), despite having lower binding energy, lacks halogen interactions, leading to weaker activity. $\mathbf{E_7}$ (-8.8 kcal/mol) shares the same binding site as $\mathbf{E_2}$ and, despite not forming halogen bonds, still exhibits good activity. $\mathbf{E_{11}}$, with the lowest binding energy (-9.7 kcal/mol), demonstrates the strongest interactions and the highest inhibitory potential.

3.2. Synthesis and bioactivity of compounds containing 1,2,4-triazole heterocycles

3.2.1. Synthetic

Compounds containing 1,2,4-triazole heterocycles were also synthesized from 2-(naphthalen-1-yl)acetohydrazide (**B**) as shown in Figure 2.1.

3.2.1.1. Synthetic processes

- Synthesis of compound (**F**) is presented in section 2.3.3.1 of the thesis.

- Synthesis of compound (**G_{1-9}**) presented in section 2.3.3.2 of the thesis.

- Synthesis of compound (**H_{1-5}**) presented in section 2.3.3.3 of the thesis.

- Synthesis of compound (**I**) is presented in section 2.3.3.4 of the thesis.

- Synthesis of compound (**J_{1-7}**) is presented in section 2.3.3.5 of the thesis.

- Synthesis of compound (**K_{1-5}**) presented in section 2.3.3.6 of the thesis.

Compound series **G**, **H**, **J**, **K** were synthesized by S_N2 substitution reaction with *N*-aryl-2-chloroacetamide in acetone solvent or 2-bromo-1-aryl/coumarine ethanone in ethanol solvent.

3.2.1.2. Result

- Synthesis of compound (**F**) is presented in section 3.3.1 of the thesis.

- The synthesis of the series of compounds (**G_{1-9}**) is presented in table 3.3. The IR, ^{1}H-NMR, ^{13}C-NMR and HR-MS spectral data are presented in tables 3.18 to 3.21 of the thesis. The single crystal X-ray diffraction results of compounds **G_1**, **G_3** and **G_9** are presented in figures 3.39, 3.40, 3.41 of the thesis and the basic parameters of the crystal lattice are presented in table 3.22 of the thesis.

Table 3.3. Results of synthesis of compounds (G_{1-9})

Comps.	Solvent recrystallize	Melting point (^oC)	Status – color	Yield (%)
G_1	EtOH : H_2O	168	White needle-shaped crystals	70.0
G_2	EtOH : H_2O	127	White needle-shaped crystals	72.1
G_3	EtOH : H_2O	155	White needle-shaped crystals	79.9
G_4	EtOH : H_2O	97	White needle-shaped crystals	73.5
G_5	EtOH : H_2O	124	White needle-shaped crystals	66.1
G_6	EtOH : H_2O	175	White needle-shaped crystals	69.1
G_7	EtOH : H_2O	192	White needle-shaped crystals	61.5
G_8	EtOH : H_2O	187	White needle-shaped crystals	87.9
G_9	EtOH : H_2O	175	Yellow needle-shaped crystals	84.8

- The synthesis of the series of compounds (**H_{1-5}**) is presented in table 3.4. The IR, ^{1}H-NMR, ^{13}C-NMR and HR-MS spectral data are presented

from table 3.31 to table 3.34 of the thesis. The single crystal X-ray diffraction results of compound **H_4** are presented in Table 3.35, Figure 3.52 of the thesis.

Table 3.4. Results of synthesis of compounds (H_{1-5})

Comps.	Solvent recrystallize	Melting point (°C)	Status – color	Yield (%)
H_1	EtOH : H_2O	166	White needle-shaped crystals	77.3
H_2	EtOH : H_2O	160	White needle-shaped crystals	80.6
H_3	EtOH : H_2O	172	Yellow needle-shaped crystals	78.9
H_4	EtOH : H_2O	182	Yellow needle-shaped crystals	76.8
H_5	EtOH : H_2O	196	Brownish yellow needle-shaped crystals	77.3

- Synthesis of compound (**I**) is presented in section 3.3.1 of the thesis.

- The synthesis of the series of compounds (**J_{1-7}**) is presented in Table 3.5. The IR, ^{1}H-NMR, ^{13}C-NMR and HR-MS spectral data are presented in Tables 3.18 to 3.21 of the thesis. The single crystal X-ray diffraction results of compounds **J_4** and **J_5** are presented in table 3.26, Figures 3.42 and 3.43 of the thesis.

Table 3.5. Synthesis of compounds (J_{1-7})

Comps.	Solvent recrystallize	Melting point (°C)	Status – color	Yield (%)
J_1	EtOH : H_2O	14 1	Needle-shaped, white crystals	91.0
J_2	EtOH : H_2O	147	White needle-shaped crystals	59.5
J_3	EtOH : H_2O	152	White needle-shaped crystals	64.0
J_4	EtOH : H_2O	14 9	White needle-shaped crystals	43.8
J_5	EtOH : H_2O	18 3	White needle-shaped crystals	41.5
J_6	EtOH : H_2O	213	White crystals	49.2
J_7	EtOH : H_2O	185	Brown flaky crystals	56.3

- The synthesis of the compound series (**K_{1-5}**) is presented in table 3.5. The IR, ^{1}H-NMR, ^{13}C-NMR and HR-MS spectral data are presented in tables 3.31 to 3.34 of the thesis.

Table 3.6. Results of synthesis of compounds (K_{1-5})

Comps.	Solvent recrystallize	Melting point (°C)	Status – color	Yield (%)
K_1	EtOH : H_2O	154	White needle-shaped crystals	70.1

K_2	EtOH : H_2O	162	White needle-shaped crystals	73.6
K_3	EtOH : H_2O	164	White needle-shaped crystals	79.4
K_4	EtOH : H_2O	161	Yellow needle-shaped crystals	77.5
K_5	EtOH : H_2O	170	Yellow needle-shaped crystals	78.9

3.2.2. Structure

The first compounds contain 1,2,4-triazole heterocycles (**F** and **I)** with IR**,** ^{1}H-NMR, ^{13}C-NMR, HR-MS spectral data consistent with the expected structure. The signals on these spectra also indicate the thiol/thione forms of the above two compounds, in which the thione form is the main form. This is also confirmed through X-ray diffraction of the crystals of **F** and **I.**

a. Structures of compounds ***(G_{1-9}) and (J_{1-7})***

Compared with the IR spectra of compounds **F** and **I**, in the IR spectra of compounds **(G_{1-9})** and **(J_{1-7}),** there is no longer absorption at around 2708 cm^{-1} (thiol S–H) but there is additional strong absorption at around 1660 – 1691 cm^{-1} (in the compound series **G_{1-9}**) and 1655–1688 cm^{-1} (in the compound series **J_{1-7}**) characteristic of the C=O amide bond.

^{1}H-NMR spectrum of the compound series **G_{1-9}** and **J_{1-7}** (see example spectra of compounds **G_1** and **J_1** in Figure 3.5 and Figure 3.6 respectively), all signals appear in accordance with the expected structure. At high magnetic fields, the signal of the methylene group near the naphthalene ring gave a shift in the range of 4.44 – 4.46 ppm (in the **G_{1-9}** compound series) and 4.63 – 4.65 ppm (in **J_{1-7}**), while the signal of the remaining methylene group linked to the acetamide moiety –CONH– gave a signal in the range of 4.07 – 4.12 ppm (in the **G_{1-9}** compound series) and 4.06 – 4.18 ppm (in **J_{1-7}**).

Also at high magnetic fields, similar to compound **I**, the characteristic signals of the ethyl group attached to the triazole ring of compound series **J_{1-7}** were found at about 3.95 ppm (*quartet,* -CH_2CH_3) and about 0.98 – 1.00 ppm (*triplet*, -CH_2CH_3).

Compared with compounds **F** and **I** , the appearance of the flexible proton signal –NH– of the acetamide functional group in the range of 9.67 –

10.54 ppm (in the compound series **G_{1-9}**) and 9.95 – 10.52 ppm (in the compound series **J_{1-7}**) together with the signals of aromatic protons in the range of 6.87 – 8.22 ppm (in the compound series **G_{1-9}**) and 6.48 – 8.21 ppm (in the compound series **J_{1-7}**) proves the structure of compounds **G_{1-9}** and **J_{1-7}.** As expected, the synthesis reactions occurred successfully.

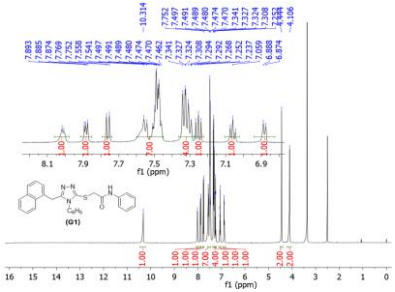

Figure 3.5. ^{1}H-NMR spectrum of compound G_1

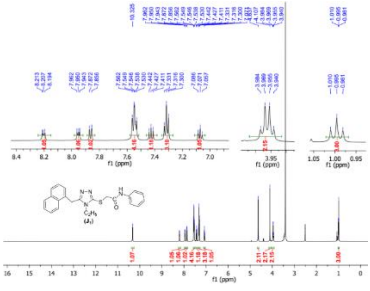

Figure 3.6. ^{1}H-NMR spectrum of compound J_1

^{13}C-NMR spectrum also showed full signals consistent with the expected structure (see for example the spectrum of compound **G_1** and **J_1** in Figure 3.7 and Figure 3.8). At low magnetic field, the carbon signal of the carbonyl group appeared in the range of 165.7 to 167.1 ppm (in the **G_{1-9}** compound series) and 165.7 to 167.3 ppm (in the **J_{1-7}** compound series). At the same time, compared with compounds **F** and **I** , the signal at around 169.0 ppm of C=S was no longer found, demonstrating the formation of the **G_{1-9}** and **J_{1-7}** compound series in the *S*-substituted form.

In the high magnetic field region, also compared with compounds **F** and **I**, additional carbon signals of the methylene group (-SCH_2CONH-) appeared in the range of 36.9 to 37.5 ppm (in the compound series **G_{1-9}**) and about 39.2 ppm (in the compound series **J_{1-7}**). Besides, the carbon signals of the ethyl group attached to the triazole ring of the compound series **J_{1-7}** also appeared at about 38.2 (-CH_2-CH_3) and 15.2 (-CH_2-CH_3).

In addition, carbon signals in the aromatic region were also found at 106.7 to 150.6 ppm (in the **G_{1-9}** series) and 106.7 to 149.2 ppm (in the **J_{1-7}**

series). In general, the signals in this region are relatively complex and some signals overlap each other, so the number of signals on the spectrum may not correspond to the number of carbon atoms in the molecule. However, the high-resolution mass spectrum HR-MS correctly represents the values of the molecular ion peaks, which allows to confirm that the compounds **G1-9** and **J1-7** have been successfully synthesized. Besides, the compounds **G1**, **G3**, **G9**, **J4**, **J5** have suitable crystals for X-ray diffraction. This result not only shows the conformity of the structure with the expected formula but also confirms the nucleophilic substitution reaction between substance **F** and *N* -aryl-2-chloroacetamide; between substance **I** and 2-bromo-1-aryl/coumarine ethanone to form the series of substances **G1-9** and **J1-7**, respectively, as *S*-substituted products rather than *N*-substituted products.

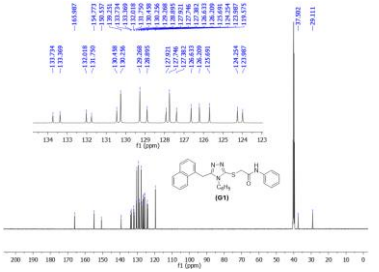

Figure 3.7. ^{13}C-NMR spectrum of compound G$_1$

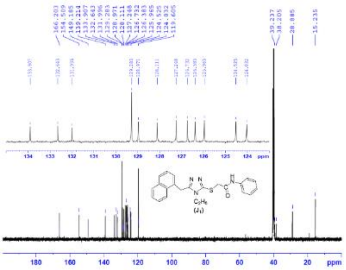

Figure 3.8. ^{13}C-NMR spectrum of compound J$_1$

High-resolution mass spectra HR-MS of compounds **G1-9** and **J1-7** show molecular ion peaks consistent with the expected structure. Single crystal X-ray diffraction also helps to study in more detail the structures of the crystals **G1**, **G3**, **G9**, **J4** and **J5** are presented in section 3.3.2.2e of the thesis. This result together with the spectral data confirms the successful synthesis of the *N*-aryl 2-{[5-(naphthalen-1-ylmethyl)-4-phenyl/ethyl-4*H*-1,2,4-triazol-3-yl]thio}acetamide **G1-9** and **J1-7** compounds.

*b. Structures of compounds **(H1-5)** and **(K1-5)***

In the IR spectrum of compounds **H1-5** and **K1-5** , all signals appeared

in accordance with the expected structure. The signal of the C=O group at 1668 – 1746 cm^{-1} showed that the substitution reaction was successful, the aryl/coumarin-3-yl acetyl moiety was attached to the 1,2,4-triazole ring. In addition, absorption peaks at 1518 – 1610 cm^{-1} (C=C, C=N), 2911 – 2987 cm^{-1} (Csp^3 –H), and 3044 – 3091 cm^{-1} (Csp^2 –H) were also observed. For compound **H_5**, the appearance of 2 signals of the C=O group at 1746 and 1730 cm^{-1} demonstrated the presence of the coumarine moiety.

^{1}H-NMR spectrum of the compound series **H_{1-5}** and **K_{1-5}** (see example spectra of compounds **H_1** and **K_1** in Figure 3.9 and Figure 3.10, respectively), all signals appear in accordance with the expected structure.

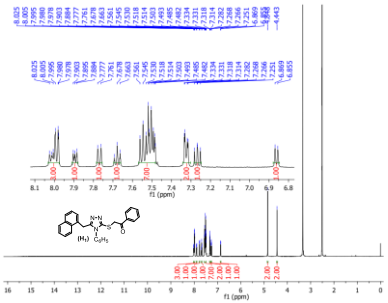

Figure 3.9. ^{1}H-NMR spectrum of compound H_1

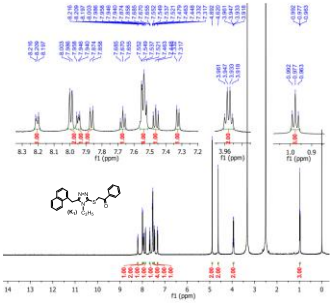

Figure 3.10. ^{1}H-NMR spectrum of compound K_1

Similar to the compounds in series **G_{1-9}** and **J_{1-7}**, the signal of the methylene group attached to the naphthalene ring appeared at 4.43 – 4.62 ppm, while the signal of the remaining methylene group (-SCH_2C =O) appeared in the *singlet* form at a higher shift, about 4.73 – 4.97 ppm, possibly due to the stronger electron-withdrawing effect of the carbonyl group and of sulfur. The characteristic signal of the ethyl group attached to the 1,2,4-triazole ring in series **K_{1-5}** were also observed similar to the signals appearing in the compound series **J_{1-7}**, specifically the *quartet* signal at 3.94 ppm and the *triplet* signal at 0.98 ppm. The aromatic region signals appeared fully protonated at 6.85–8.74 ppm but, like compounds **G_{1-9}** and **J_{1-7}**, were

complex, overlapping, and shown as *multiplets*.

^{13}C-NMR spectrum shows all the signals consistent with the expected structure (see for example the spectrum of compound **H$_1$** and **K$_1$** in figure 3.11 and 3.12). Similar to the series of compounds **G$_{1-9}$** and **J$_{1-7}$** , the disappearance of the thione carbon (C=S) signal in compounds **F** and **I** (δ 166.8–168 ppm) demonstrates the formation of compounds **H$_{1-5}$** and **K$_{1-5}$** in the *S*-substituted form. At low magnetic fields, the carbonyl group carbon signal appears at 191.0–193.8 ppm. The triazole C=N carbon and aromatic carbon signals appear at 150.0–154.8 ppm and 124.6–140.6 ppm, respectively, with slight changes in the shift depending on the nature of the substituent. Signals of the methylene carbon and the ethyl carbon are also found at 15.2–43.6 ppm.

High-resolution mass spectra HR-MS of compounds **H$_{1-5}$** and **K$_{1-5}$** show molecular ion peaks consistent with the expected structure. The single crystal X-ray diffraction method also helps to study in more detail the structure of the **H$_4$** crystal presented in section 3.3.3.2e of the thesis. This result together with the spectral data confirms the successful synthesis of the compound series 2-{[5-(naphthalen-1-ylmethyl)-4-phenyl-4*H*-1,2,4-triazol-3-yl]thio}-1-aryl/coumarin-3-yl ethan-1-one (**H$_{1-5}$**) and 2-{[5-(naphthalen-1-ylmethyl)-4-ethyl-4*H*-1,2,4-triazol-3-yl]thio}-1-aryl ethan-1-one (**K$_{1-5}$**).

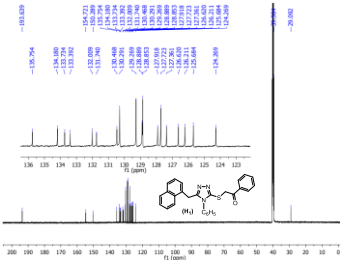

Figure 3.11. ^{13}C-NMR spectrum of compound H$_1$

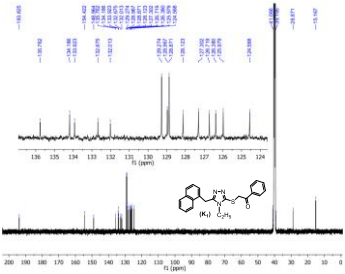

Figure 3.12. ^{13}C-NMR spectrum of compound K$_1$

3.2.3. α-glucosidase enzyme inhibitory activity

Compounds containing 1,2,4-triazole heterocycles showed superior α-glucosidase inhibitory activity, with IC_{50} from 0.11 ± 0.04 to 345.67 ± 0.09 μM, better than voglibose (IC_{50} = 355.8 ± 3.5 μM). However, the **J_{1-6}** series did not show activity, the results are presented in Table 3.7 and Figure 3.13.

Table 3.7. α-Glucosidase inhibitory activity of compound series G, H, J, and K

Comps.	R	IC_{50} (μM)	Binding energy (kcal/mol)	Hydrogen bond
F		15.11 ± 0.11	-8.1	-
G_1	H	21.89 ± 1.28	-8.5	Asn352
G_2	2-CH_3	0.11 ± 0.04	-9.9	Arg404
G_3	4-CH_3	8.68 ± 0.25	-9.7	Asn352
G_4	3-Cl	7.71 ± 1.56	-9.8	Asn352
G_5	4-Cl	7.32 ± 0.98	-9.4	Asn352
G_6	4-Br	5.90 ± 0.14	-9.4	Asn352
G_7	4-OCH_3	0.33 ± 0.07	-8.9	Asn352
G_8	3-OH	0.19 ± 0.04	-9.0	Asn352
G_9	4-NO_2	4.56 ± 0.21	-9.4	Asn352
J_1	H	-	-8.9	Asp73, Asp420
J_2	4-CH_3	-	-8.4	-
J_3	4-OCH_3	-	-8.2	-
J_4	2-Cl	-	-8.7	-
J_5	4-Cl	-	-8.4	-
J_6	4-NO_2	-	-8.0	-
J_7	3-OH	158.4 ± 3.4	-9.3	Asp197
H_1	H	65.69 ± 0.09	-9.8	Arg404
H_2	4-Cl	9.23 ± 0.04	-9.6	Arg404
H_3	4-Br	9.61 ± 0.06	-9.7	Arg404
H_4	4-NO_2	21.16 ± 0.06	-9.5	His478
H_5	Coumarin-3-yl	25.41 ± 0.06	-10.5	Arg404
K_1	-H	312.12± 0.08	-9.4	Arg404
K_2	4-Cl	177.82 ± 0.17	-9.0	Arg404
K_3	4-Br	223.77 ± 0.13	-9.0	Arg404
K_4	4-NO_2	38.30 ± 0.16	-9.1	His478
K_5	3-NO_2	345.67 ± 0.09	-9.4	His478
Voglibose		355.8 ± 3.5		

The series of compounds (**F**, **G**$_{1\text{-}9}$) exhibited superior activity with IC_{50} ranging from 0.11 to 21.89 μM, significantly higher than that of voglibose and the series (**I**, **J**$_{1\text{-}7}$). Compound **G**$_2$ (2-CH_3) had the strongest activity (IC_{50} = 0.11 μM), indicating the effect of the small electron-donating substituent, while **G**$_8$ (3-OH) and **G**$_7$ (4-OCH_3) also showed high activity. The halogen-containing compounds showed moderate activity, with **G**$_6$ (4-Br) being more active than **G**$_4$ (3-Cl) and **G**$_5$ (4-Cl), while **G**$_9$ (4-NO_2) showed better activity than the halogen group due to its strong electron-withdrawing effect. In contrast, the series (**I**, **J**$_{1\text{-}7}$) showed lower activity, with only **J**$_7$ (3-OH) showing activity but still low. This result confirms the potential of 4-phenyl-4*H*-1,2,4-triazole in the development of α-glucosidase inhibitors when suitable substituents are used.

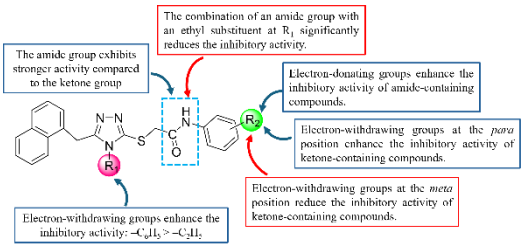

Figure 3.13. Structure–activity relationship of compound series G, H, I, and J containing a 1,2,4-triazole ring

Docking results showed that compound **G**$_2$ had the best activity due to the lowest binding energy (-9.9 kcal/mol) and stable interactions with the enzyme, including hydrogen bonding with Arg404 and hydrophobic interactions with Phe314, Val351. **G**$_7$ (-8.9 kcal/mol) and **G**$_8$ (-9.0 kcal/mol) also had strong interactions, especially hydrogen and π–π bonding with Trp169, Phe314. Compound **J**$_7$ had good binding energy (-9.3 kcal/mol) but low activity (IC_{50} = 158.4 μM), possibly due to differences in the location and type of interactions in the binding cavity (see Figure 3.14).

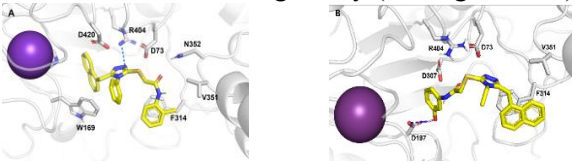

Figure 3.14. Docking poses of compounds G$_2$ (A) and J$_7$ (B)

Compounds **H**$_{1-5}$ exhibited superior α-glucosidase inhibitory activity compared to voglibose, with **H**$_2$ (4-Cl) and **H**$_3$ (4-Br) having IC_{50} values of about 9.2–9.6 μM, 37 times more potent than voglibose, indicating the active role of the electron-withdrawing substituent. **H**$_4$ (4-NO_2) and **H**$_5$ (coumarin-3-yl) also had good activity, although lower than **H**$_2$ and **H**$_3$, while **H**$_1$ no substituents on the benzene ring still achieved significant inhibitory effect. The **K**$_{1-5}$ series also showed better activity than voglibose, with **K**$_4$ (4-NO_2) being the most potent (IC_{50} = 38.3 μM), but was generally less active than the **H**$_{1-5}$ series (see Figure 3.15).

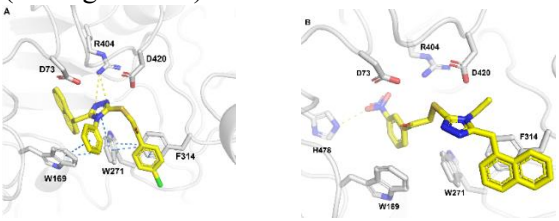

Figure 3.15. Docking poses of compounds H$_2$ (A) and K$_4$ (B)

Molecular docking results showed that compounds **H**$_2$ and **H**$_3$ had the best activity in the **H**$_{1-5}$ series although their binding energy was not the lowest (-9.6 and -9.7 kcal/mol). They formed hydrogen bonds with Arg404 and π–π interactions with Trp169, Phe314, helping to stabilize the enzyme-ligand complex. **H**$_1$ (-9.8 kcal/mol) had lower activity due to unfavorable orientation, which lost the important π–π interaction. **H**$_5$ (-10.5 kcal/mol) had the lowest binding energy but its activity was not superior.

In the **K**$_{1-5}$ series, **K**$_2$ and **K**$_3$ (-9.0 kcal/mol) have good binding energy but weak activity. **K**$_1$ (-9.4 kcal/mol) has higher binding energy but still low activity. **K**$_4$ (-9.1 kcal/mol) interacts with His478 and Phe314 but lacks binding with Trp169, reducing the inhibitory effect.

CONCLUSION AND RECOMMENDATIONS

1. Conclusion

1.1. Synthesis and structural research

Starting from 2-(naphthalen-1-yl)acetic acid, a total of 42 compounds were synthesized, including:

- Ethyl 2-(naphthalen-1-yl)acetate.
- 2-(Naphthalen-1-yl)acetohydrazide (**B**).
- 2-(Naphthalen-1-yl)-*N*-(4-oxo-2-thioxothiazolidin-3-yl)acetamide (**D**).
- 5-(Naphthalen-1-ylmethyl)-4-phenyl-4*H*-1,2,4-triazole-3-thiol/thione (**F**).
- 4-Ethyl-5-(naphthalen-1-ylmethyl)-4*H*-1,2,4-triazole-3-thiol/thione (**I**).
- 11 compounds *N*-(5-arylidene/piperonylidene-4-oxo-2-thioxothiazolidin-3-yl)-2-(naphthalen-1-yl)acetamide (**E$_{1-11}$**).
- 09 compounds *N*-aryl compounds 2-{[5-(naphthalen-1-ylmethyl)-4-phenyl-4*H*-1,2,4-triazol-3-yl]thio}acetamide (**G$_{1-9}$**).
- 05 compounds 2-{[5-(naphthalen-1-ylmethyl)-4-phenyl-4*H*-1,2,4-triazol-3-yl]thio}-1-aryl/coumarin-3-yl ethanone (**H$_{1-5}$**).
- 07 compounds *N*-aryl compounds 2-{[5-(naphthalen-1-ylmethyl)-4-ethyl-4*H*-1,2,4-triazol-3-yl]thio}acetamide (**J$_{1-7}$**).
- 05 compounds 2-{[5-(naphthalen-1-ylmethyl)-4-ethyl-4*H*-1,2,4-triazol-3-yl]thio}-1-aryl ethanone (**K$_{1-5}$**).

Among the synthesized compounds, 39 are novel (as identified in SciFinder, August 2025), comprising heterocyclic compounds incorporating both 2-thioxothiazolidin-4-one and 1,2,4-triazole scaffolds, specifically **D**, **I**, **E$_{1–11}$**, **G$_{1–9}$**, **H$_{1–5}$**, **J$_{1–7}$**, and **K$_{1–5}$**.

The structures of all compounds were confirmed by their IR, ^{1}H-NMR, ^{13}C-NMR, HR-MS spectral data. Particularly compounds **D**, **E$_4$**, **E$_8$**, **F**, **G$_1$**, **G$_3$**, **G$_9$**, **I**, **J$_4$**, **J$_5$** and **H$_4$** were also structurally investigated by single crystal X-ray diffraction analysis.

1.2. Biological activity

- All heterocyclic compounds (except **D**, **E_5**, **E_8**, **F**, **J_{1-6}**) exhibited moderate to good activity, surpassing voglibose (IC50 = 355.8 ± 3.5 μM) as the positive control.

- The structure–activity relationship (SAR) study shows that 1,2,4-triazole exhibits stronger α-glucosidase inhibition than 2-thioxothiazolidin-4-one. Electron-withdrawing groups (-NO_2, -Cl, -Br) enhance inhibition, while electron-donating groups (-CH_3, -OCH_3) have a position-dependent effect.

- The IC_{50} values from 7.5 ± 0.5 μM to 290.3 ± 1.9 μM of series **E**. Compound **E_2** showed the best activity, compound **D** did not show activity, indicating that the substituent group at position 5^{th} on the thiazolidine heterocycle greatly affected the activity.

- The IC_{50} values from 0.11 ± 0.04 μM to 345.67 ± 0.09 μM of the compounds containing 1,2,3-triazole. Among these compounds, the compound containing the phenyl group on the 1,2,4-triazole heterocycle showed better activity, the best being compound **G_2**. Compound **I** containing the ethyl group on the 1,2,4-triazole heterocycle did not show activity, which also affected its derivatives to show weaker activity or even no activity.

- Molecular docking methods also showed the stability of the synthesized compounds in the binding site of the enzyme α-glucosidase (PDB ID: 6C9X) by hydrogen bonds with key amino acids such as Arg404, Asp73, Asp197, Asn352 and π-π interactions with Trp169 and Phe314.

2. Recommendations

- Investigate antibacterial, antifungal, antioxidant, and anticancer activities.
- Optimize synthesis using catalysts or microwave-assisted reactions.
- Synthesize new heterocycles (1,3,4-oxadiazole, 4-amino-1,2,4-triazole,…) and evaluate their bioactivity.

LIST OF THE PUBLICATIONS RELATED TO THE DISSERTATION

1. **Trong Duc Le**, Tien Cong Nguyen, Thi My Nuong Bui, Thi Kim Dung Hoang, Quoc Trung Vu, Chien Thang Pham, Chau Phi Dinh, Jibril Abdullahi Alhaji, and Luc Van Meervelt. 2023. "Synthesis, Structure and α-Glucosidase Inhibitor Activity Evaluation of Some Acetamide Derivatives Starting from 2-(Naphthalen-1-yl) Acetic Acid, Containing a 1,2,4-Triazole." *Journal of Molecular Structure* 1284:135321. (SCIE, Q2, IF 3.8).

2. **Trong Duc Le**, Tien Cong Nguyen, Thi Kim Dung Hoang, Minh Khoi Huynh, Quang Thang Phan, and Luc Van Meervelt. 2024. "Synthesis, Crystal Structure and Hirshfeld Surface Analysis of 2-({5-[(Naphthalen-1-yl)Methyl]-4-Phenyl-4*H*-1,2,4-Triazol-3-yl}sulfanyl)-1-(4-Nitrophenyl) Ethanone." *Acta Crystallographica Section E* 80(2):218–22. (ESCI, Q3).

3. **Trong Duc Le**, Tien Cong Nguyen, Thi Minh Dinh Tran, Thi Kim Dung Hoang, Khanh Duong To, Minh Phuong Hien Nguyen, Thi My Ngan Tran, Chau Phi Dinh, Jibril Abdullahi Alhaji, and Luc Van Meervelt. 2024. "Studying the Structure and Evaluating α-Glucosidase Inhibition of Novel Acetamide Derivatives Incorporating 4-Ethyl-4*H*-1,2,4-Triazole Starting from 2-(Naphthalen-1-yl)Acetic Acid." *Asian Journal of Organic Chemistry* 13(6):e202400063. (SCIE, Q2, IF 3.3).

4. Tien Cong Nguyen, **Trong Duc Le**, Thi Kim Dung Hoang, Chien Thang Pham, Jibril Abdullahi Alhaji, Thi Chi Nguyen, Ngoc Anh Truong, Chau Phi Dinh, and Luc Van Meervelt. 2025. "Synthesis, Evaluation of α-Glucosidase Inhibitory and Antimicrobial Activities of Novel *N*-(5-Arylidene-4-Oxo-2-Thioxothiazolidin-3-yl)-2-(Naphthalen-1-yl)Acetamide Derivatives." *Journal of Molecular Structure* 1326:141068. (SCIE, Q2, IF 4.0).

5. Cong T. Nguyen, Dung T.K. Hoang, Vu A. Truong, Loan T.K. Nguyen, Phi C. Dinh, Dung H.A. Mai, **Duc T. Le**, and Nam N. Pham. 2025. "Synthesis and *In Vitro/In Silico* α-Glucosidase Inhibitory Study of Novel Ethanones Containing Naphthalene-Linked 1,2,4-Triazole." *ACS Medicinal Chemistry Letters.* doi: 10.1021/acsmedchemlett.5c00387. (SCIE, Q1, IF 4.0).